Proceedings of the Canadian Society for Mechanical Engineering International Congress 2022
CSME Congress 2022
June 5-8, 2022, Edmonton, AB, Canada

Wind-Driven Rain Effects on Automotive Camera and LiDAR Performances

Wing Yi Pao[1*], Long Li[2], Martin Agelin-Chaab[1]
[1]Department of Mechanical and Manufacturing Engineering, Ontario Tech University, Oshawa, Canada
[2]Department of Automotive and Mechatronics Engineering, Ontario Tech University, Oshawa, Canada
*wingyi.pao@ontariotechu.net

Abstract— Modern vehicles are equipped with Advanced Driver Assistance Systems (ADAS) that rely heavily on a variety of sensors such as LiDAR, RADAR, SONAR, and camera to capture surrounding traffic data. Sensor performance has been observed to degrade during adverse weather conditions as the signals are attenuated due to soiling on the external surfaces of the sensor. This poses huge risks to both occupants and pedestrians. In order to improve the safety of ADAS, it is essential to understand and quantify the effects of soiling on sensor signals. This paper investigates driving-in-rain scenarios, which are some of the most ubiquitous but hazardous weather conditions that cause accidents every year due to reduced driver and sensor vision. Rain was simulated in a controlled environment onto an automotive external camera and a single-point LiDAR in a wind tunnel. Perceived soiling characteristics when the vehicle is moving at different speeds under different natural rain intensities are considered and measured, including impact, intensity, velocity, and droplet size distribution. Sensor performance is evaluated based on image processing techniques and statistical analysis on signal data. The results show that camera image degrades with both increasing rain intensity and driving speed, whereas LiDAR signal only worsens during heavier rain conditions. However, driving faster when perceived rain intensity is kept constant improves the perception with faster signal recovery.

Keywords-LiDAR; camera; sensor performance; rain simulation; perceived characteristics; autonomous vehicle; image processing; soiling quantification

I. INTRODUCTION

Advanced Driver Assistance Systems (ADAS) are increasingly being found in modern vehicles which offer various automated features, such as adaptive cruise control, emergency braking, blind-spot warning, and lane-keeping. The use of ADAS is believed to be the future of autonomous vehicles with higher level of autonomy.

ADAS consists of different types of sensors to perform ranging and imaging of the surrounding environment. Fig. 1 shows the ADAS components and their respective functions in a vehicle. A vision camera is a type of optical sensor that works in the visible light region, thus providing live images of perceptions comparable to human eyes. On the other hand, Light Detection and Ranging (LiDAR) utilizes laser and the time-of-flight (TOF) principle to detect the distance between an object and the vehicle. Using both camera and LiDAR together is suitable for short range operations to obtain the view and depth of obstacles during vehicle navigation [1]. Other typical sensors include RADAR, SONAR, and infrared camera that are also used in ADAS, but are not the focus of this study, and are thus, not discussed in this paper.

It is known that sensors degrade in performance in adverse weather conditions, as precipitation and wet ground contribute to primary and secondary soiling. Typical examples of sensor performance degradation are having false detections that cause warning and malfunction such as sudden braking, request for human inputs, etc. These situations hinder the advancement of the autonomous vehicle technology and the subsequent adoption of autonomous vehicles.

This paper focuses on rain, which is a common precipitation condition around the world, it also accounts for 50% of weather-related road accidents [2]. Furthermore, the quantifiable effect of soiling on automotive sensor performance is not very well understood, most studies in the literature lack realistic testing conditions and only simulate for natural rain characteristics, which ignore the perceived rain (the fact that the frontal area of a moving vehicle experiences more rain with increasing driving speed). This paper fills the literature gap with realistic perceived conditions reflecting what sensors see during vehicle operation in rain. We also propose various evaluation methods to quantify the amount of soiling and the resulting sensor performances. These are the data that are useful for further developments on soiling mitigation, signal correction, and the validation of numerical models.

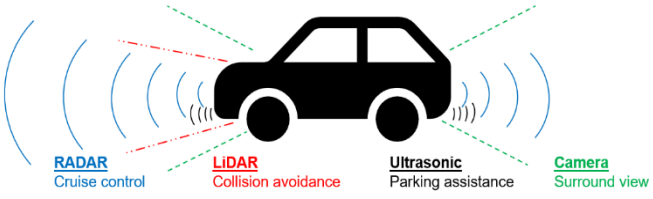

Figure 1. Sensors used in autonomous vehicles and example of their respective functions.

The objectives of this paper are to simulate realistic and controlled wind-driven rain conditions that represent what a moving vehicle experiences, as well as to study how rain intensities and driving speeds affect frontal camera and LiDAR performances. The study consists of two groups of conditions: {1} driving at the same speed but experiencing different perceived rain intensities, and {2} driving at different speeds but experiencing the same perceived rain intensities.

II. Literature Review

A. Perceived Rain Characteristics of a Moving Vehicle

Natural rain conditions are categorized based on intensity and droplet size distribution. Other perceived rain characteristics of a moving vehicle include impact angle and energy. Rain angle can be explained with analogy to the light aberration phenomenon [3] for which the apparent rain impact angle depends on the moving velocity of the vehicle, such that a driver and frontal sensors would see the rain tilts and falls behind when driving forward.

Droplet size distribution is the end product of various events before raindrops impact, namely breakup, collision, and coalescence [4]. Droplet size distribution is independent of driving speeds as droplet dynamics are assumed to be unaffected by the movement of the vehicle. However, the frontal area of a moving vehicle experiences more raindrops per unit time at higher driving speeds due to increase in flux as suggested by Bocci [5], hence higher perceived rain intensity as compared to the intensity that is experienced by a stationary vehicle.

B. Camera Performance in Rain

When the outer surface of the camera is exposed to raindrops, where the surface may be a protective cover or the camera lens itself, the image is blurry or distorted. In severe cases, the objects in the image frame can be overlapped by rain droplet. The mentioned problems directly result in performance degradation of the ability to accurately detect and identify distanced objects when driving in rain [6].

The behavior of light refraction through a raindrop was studied and modeled by Roser, et al. [7]. The focus quality of an image under the influence of raindrops depends on the thickness of the droplet at the respective location. With reference to the blur map of an image caused by a single droplet, attempt was made by Parov, et al. to restore an image under the influence of rain [8]. The influence of an image frame captured by optical camera can be generalized and categorized into two parts – raindrops in mid-air, and droplets adhering to camera outer surface. However, Parov and Roser both were using simulated droplets through controlled experiments or computer simulations; hence the droplet behavior does not coincide with realistic driving-in-rain observations. Both stated the need to recreate realistic, yet controlled rain intensity and droplet distribution.

A more detailed investigation on the magnitude of rain intensity at various driving conditions is much needed. In driving-in-rain conditions where optical camera outer surface is bombarded by raindrops at a high frequency, the ability to detect and predict object and its movement decreases significantly. Presence of droplets at the camera surface results in combinations of blurriness, distortion, and blockage of objects in the image frame [9].

Currently, to combat blurriness of an image frame, autofocus systems are commonly built into camera hardware based on various algorithm methods. However, the frequency and variability of droplets present on the camera outer surface exceed the capability of existing passive autofocusing algorithms [10]. Subbarao, et al. investigated different methods to optimize image focus measure for isolated-image passive autofocus systems [11]. The study of Subbarao deduced that the focus quality of the image, in conjunction with the autofocusing error, is highly dependent on the grayscale level noise and the image content. When droplet is present at the outer surface of camera in rain, the image content is altered due to the fact that those droplets are considered to be at the foreground of the respective image frame. If the focus level of the camera is fixed to the background environment, the grayscale noise intensity increases, reducing the focus quality of the image.

The ability to detect object and predict object movement in real time were studied by Guan, et al. [12]. Live object tracking presents even greater difficulty compared to isolated image passive autofocusing because of the constant unpredictable changes in image focus quality due to rain droplets. The accuracy and the predictability in object detection are highly dependent on the focus quality of each image frame. Camera performance degrades dramatically in heavy rain conditions, most current live object detection algorithms do not have the ability to provide object detection and tracking. Therefore, it is important to understand the effects of different driving-in-rain conditions on camera focus quality, such that adequate algorithms can be developed.

C. LiDAR Performance in Rain

LiDAR works via an echo time-of-flight principle, as stated in (1), where *D*, *c*, and *t* represent distance, speed of light, and time, respectively. The sensor emitter sends out short-pulsed laser beam of known wavelength and energy, and measures the power and time it takes for the return beam to reach the receiver. The relationship between laser signal power, *P*, and range of detected object, *Z*, is stated in (2) [13], where the return signal strength is inversely proportional to the square of range.

$$D = c \cdot t/2 \tag{1}$$

$$P_{returned} \propto P_{transmitted} \cdot \frac{1}{Z^2} \tag{2}$$

Rain studies for LiDAR are on the rise with increasing interest in autonomous technology. Filgueira, et al. investigated the effects of rain on a 3D scanning LiDAR. Using an outdoor stationary LiDAR setup, it was found that detected range was stable with only up to about 10% fluctuation for all six targets of different materials, but the measured intensity and number of points were reduced with increasing rain intensity [14].

The major reason for sensor performance degradation in rain is due to signal attenuation, resulting in inaccurate ranging.

Laser that passes through a raindrop in air may result in total deflection and false detection [15]. The relationship between rainfall rate and atmospheric attenuation coefficient, α, follows a power law, as shown in (3) [13, 16]. The return power is affected by the attenuation coefficient as stated by (4), and the constant values c_1 and c_2 are determined experimentally and are dependent on LiDAR parameters.

$$\alpha = c_1 R^{c_2} \quad (3)$$

$$P_{returned} \propto e^{-2\alpha Z} \quad (4)$$

Equation (3) and (4) only assume LiDAR sensing through a homogeneous and uniform scattering medium, meaning there are no considerations of droplets that appear on the sensor surface close to the laser aperture. In this situation, power intensity is altered in the return signal [15]; this is a realistic scenario that cannot be neglected when a moving vehicle hits through a volume of rain.

Zhang, et al. investigated on board LiDAR performance at a 2 km route with pre-built scanning map [17]. The number of reconstructed space points in the point-cloud reduces significantly with increasing rain intensity. However, they only performed low speed experiments up to 35 km/hr. In order to establish a complete driving-in-rain model for automotive LiDAR, more on-board and controlled lab test datasets are needed, which is currently lacking in the literature.

III. EXPERIMENTAL

A small-scale wind tunnel was employed for simulation of wind-driven rain. The effects of three different perceived rain intensities and driving speeds were studied, leading to a 3 by 3 matrix of 9 conditions in total. Rain characteristics for each case were quantified and the same conditions were simulated onto a camera and a LiDAR. Control measurements were taken without rain and wind for 30 seconds. Each condition was run for 2 min when a steady state of wind and rain was reached. Each condition was repeated to ensure repeatability via flow rate control. Analysis was performed on the average of the extracted quantitative values from the sensor signal data.

A. *Wind Tunnel*

This is an open-circuit push-down type wind tunnel that uses a centrifugal fan. This type of wind tunnel is suitable for soiling testing where contaminants are not sucked into the fan. The dimensions of the test section are 0.4 m (H) x 0.5 m (W) x 1.1 m (L).

Flow collector was in place at the top and the two sides were open to the atmosphere. This setup selection was to accommodate the rain system and the rain measurement equipment to minimize aerodynamic blockage effect. The sensors were placed side-by-side inside a waterproof container which has a frontal area 12% of the test section cross-sectional area. The container was mounted onto the bottom board and at the end of the test section. The setup is depicted by Fig. 2A. Since the study focuses on frontal soiling of sensors, the aerodynamics of the container is ignored.

B. *Rain Conditions*

Rain conditions were simulated based on the concept of Pao's numerical work [4] where water was dispensed from an elevated height, the wind then induced further breakups and deflected the droplets towards the sensors.

Perceived intensities and volume mean droplet size (D30) that were simulated for different driving speeds and natural rain conditions are presented in Table 1 and Table 2, respectively. These rain characteristics were measured using the Thies laser precipitation monitor, shown in Fig. 2B, capable of tracing each droplet that passes through the disdrometer laser beam which has a detection area of 4560 mm^2. Droplet that passes through the laser beam causes a reduction in amplitude in the receiving signal which correlates to droplet size. The duration of the diminished signal is used to calculate speed [18].

The perceived intensities increase in two directions - driving faster or increasing natural rain intensity. The ratio between perceived and natural rain intensity at different driving speeds are 1.4, 4.0, and 10.0 for 50, 75, and 100 km/hr, respectively. The selected driving speeds represent city, sub-urban, and highway speeds. For comparison, the target intensity moving along the diagonal of Table 1 from bottom left to top right was set to be the same.

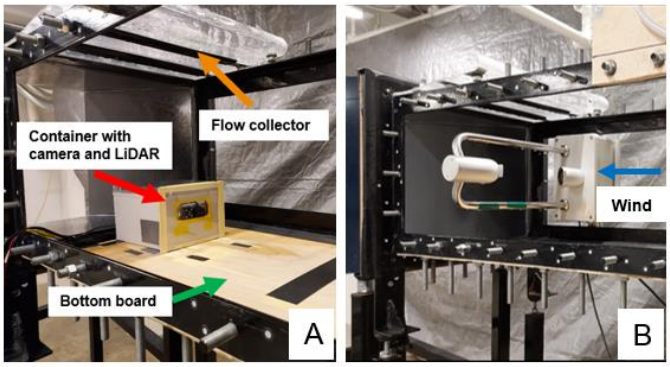

Figure 2. Wind tunnel setups for (a) sensors and (b) disdrometer.

TABLE I. PERCEIVED RAIN INTENSITIES SIMULATED FOR DIFFERENT DRIVING-IN-RAIN CONDITIONS

Rain Category	Simulated Rain Intensities (mm/hr)[a]		
	50 km/hr	*75 km/hr*	*100 km/hr*
Light	5.7	15.2	33.5
Moderate	17.4	33.1	106.5
Heavy	32.7	107.6	194.4

a. Rain intensities were experimentally measured, within ± 2 mm/hr from targeted intensities.

TABLE II. VOLUME MEAN DROPLET SIZE SIMULATED FOR DIFFERENT DRIVING-IN-RAIN CONDITIONS

Rain Category	Simulated Volume Mean Droplet Size (mm)[b]		
	50 km/hr	*75 km/hr*	*100 km/hr*
Light	0.67	0.78	0.79
Moderate	0.68	0.79	1.17
Heavy	0.79	1.18	1.46

b. D30 droplet sizes were experimentally measured.

The D30 droplet size increases with increasing rain intensities, due to the increased probability of events such as breakup, collision, and coalescence. The trend was evident by noting the smallest size found for 50 km/hr light rain condition, and largest size found for 100 km/hr heavy rain condition. The impact angle selected for all cases lied within 70º – 75º. The mean droplet velocities measured reflect the terminal velocity of droplets between 25-32 km/hr, this is a limitation of wind-driven rain, which cannot simulate for a vehicle driving into the raindrop at its driving speed.

C. Sensors

Short-range sensors were selected for this study, including a generic automotive external camera and a single-point LiDAR. The camera has a field-of-view (FOV) of 140° and resolution of 640 x 480 pixels at 20 frames-per-second. The LiDAR emits pulsed laser beam at 850 nm wavelength and has a FOV of 2°. It measures for distance and signal strength at 100 Hz. The LiDAR has an operation range between 0.2 - 8 m, with ± 2% accuracy at over 3 m distance. The simplicity and non-point-cloud based nature of this LiDAR is suitable for fundamental studies on laser interactions with raindrops.

A 1 mm thick extruded transparent acrylic cover was placed in front of the sensors without a gap, such that the sensors were not directly exposed to raindrops, but had a protective cover. The cover was used as received without coating treatments, the water contact angle (WCA) was measured to be 62° and is considered to be hydrophilic (WCA < 90°). The control frames were taken with the cover installed, thus the optical properties of the cover can be neglected.

1) Camera performance evaluation: Image processing techniques were employed to objectively quantify the accuracy and clarity of camera during various driving-in-rain conditions. The optical camera footage was converted into 16-bit grayscale snapshots. A method of Microscope Image Focus Quality (MFQ), developed by Yang's team, evaluates the focus quality of the image snapshot [10]. The image was subdivided into 9 by 7 independent grids to be examined by the method using an open source image processing package, Fiji [19]. The method employs pre-trained deep neural network to predict image snapshots in isolation. Analyzing optical camera footages using the MFQ method resulted in a difference in the overall level of in-focus grid segment between various perceived rain conditions.

2) LiDAR performance evaluation: Rain effects on signal strength were not investigated in this paper. Each experiment collected 12000 data points over 2 minutes. LiDAR was evaluated based on its ability to determine the distance to a target of a known position under various driving-in-rain conditions. The data was plotted against measured distances. Any fluctuation of measured distances from the known target distance indicates LiDAR is being affected by raindrops. The distance errors were divided into 10 groups of distance differences from the known target distance, each group is accounted for 10% increment. Error counts for less than 2% were ignored as that lied within the accuracy of the studied LiDAR. The raw data was sorted according to the 10 groups and the error frequencies were recorded. The overall performance of the LiDAR is reflected in the relative area under the error intensity curve. The area indicates the extent of the LiDAR being affected by raindrops, a lower value would mean less errors and better performances.

IV. Results and Discussions

A. Camera Performance in Rain

The raw image, 16-bit grayscale, MFQ, and gamma corrected examples are shown in Fig. 3. The gamma correction factor was set to be 0.6 for viewing purpose in the figure. The color scheme of the box layouts indicates the focus quality of that respective region, with red being in-focus, and blue being the most out-of-focus. The MFQ data was processed in raw form prior to gamma correction.

The MFQ of control frame and three examples including 50 km/hr light rain, 75 km/hr moderate rain, and 100 km/hr heavy rain are shown in Fig. 4. As seen in Fig. 4A, the control frame post-processed result shows the image as completely in-focus with a high level of confidence. As the perceived rain intensity increases from 50 km/hr light rain to 100 km/hr heavy rain, more and more boxes indicate a shift towards blue on the RGB spectrum – meaning out-of-focus.

The examples in Fig. 4 capture the increase in both perceived rain intensity and driving speed. The examples also represent the best, median, and worst cases among the nine conditions. In a light rain and low driving speed condition, the camera was affected to a lower extent with the majority of boxes still indicating red. When both perceived intensity and driving speed were at the extreme high ends, the camera lost complete visibility with only little areas being in-focus as evident by the majority of boxes having non-red colors.

Another observation made through the post-processing of the MFQ method is that as droplet diameter increases, the magnitude of blurriness (out-of-focus) also increases proportionally. When smaller droplets are present at a higher density, which blurs a larger area of the image, this scenario would result in lower contrast across the image as compared to a scenario having fewer but larger droplets.

It is suspected that although driving faster caused droplets to translate faster across the cover in different directions, a camera has wide FOV, the translation of droplets per video frame on a hydrophilic surface was relatively small compared to the FOV. The worsening effect was dominated by the increase in perceived rain intensity when there were more droplets present on the cover, causing more light deflections.

Quantification of the MFQ data was performed by identifying the color scheme of the boxes based on its RGB value. A metric of evaluation was created to benchmark the result from every experimental case. In-focus percentage for all investigated conditions are plotted in Fig. 5. If the analyzed box indicates any shift towards the blue end of the RGB spectrum, then it is considered to be out-of-focus. The level of overall image focus quality is based solely on the number of in-focus boxes. The magnitude of blurriness is investigated at a lesser extent due to the fact that it is highly application

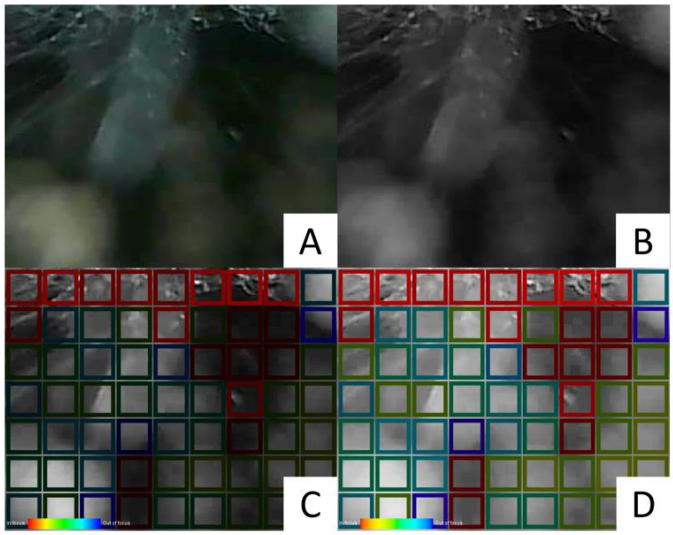

Figure 3. (a) Raw, (b) 16-bit grayscale, (c) MFQ, and (d) Gamma corrected of the same camera image frame.

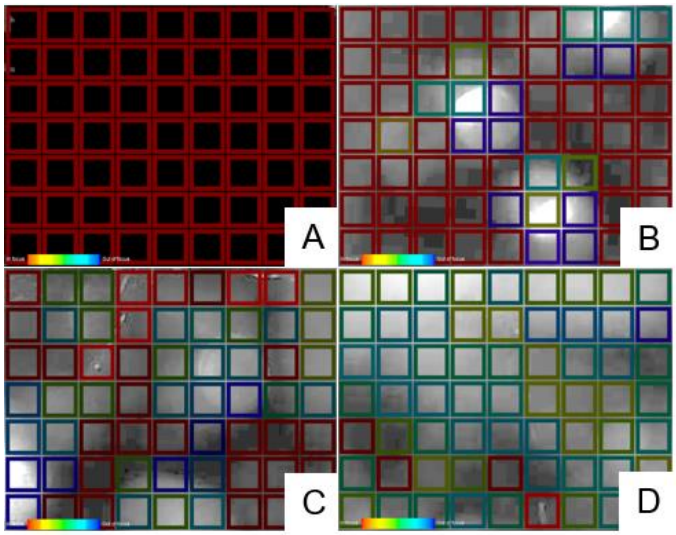

Figure 4. MFQ of (a) control frame; selected frames from (b) 50 km/hr light rain, (c) 75 km/hr moderate rain, and (d) 100 km/hr heavy rain.

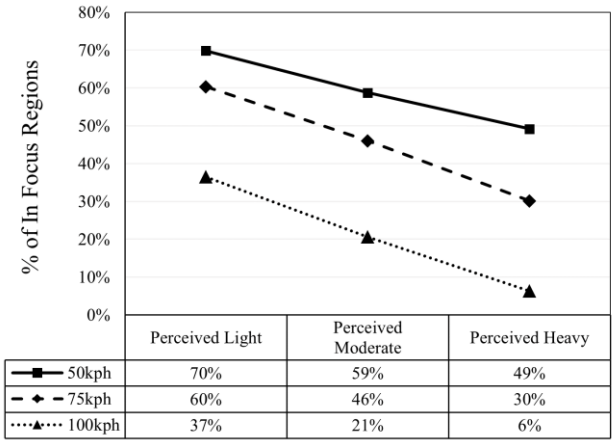

	Perceived Light	Perceived Moderate	Perceived Heavy
50kph	70%	59%	49%
75kph	60%	46%	30%
100kph	37%	21%	6%

Figure 5. Percent in focus for different driving in rain conditions.

dependent. An example can be given by comparing Fig. 4C and 4D. In Fig. 4C, larger droplets are present, indicating a greater magnitude of blurriness, yet due to its reduced droplet density, there are still in-focus areas. In Fig. 4D, although the smaller droplet size shows a reduced magnitude of blurriness, its high droplet density caused an increase in the affected area. Depending on the method to predict realistic environmental information to provide accurate and reliable road information, it is not possible to clearly state which of the example cases is worse than the other. Therefore, only the in-focus quality is quantified in this analysis.

B. LiDAR performance in Rain

LiDAR signal was affected when a droplet passes through the laser point on the protective cover. The presence of droplets in close proximity to the LiDAR resulted in inaccuracy of ranging, which deviates from the reference distance.

Fig. 6 shows the plots of detected distance for control, 50 km/hr light rain, 75 km/hr moderate rain, and 100 km/hr heavy rain; representing increase in both perceived rain intensity and driving speed. The higher frequency in distance fluctuations implies the effect of raindrops on LiDAR signal was more severe. The amount of up and down transitions was significantly higher during 100 km/hr heavy rain condition (Fig. 6D) as compared to 50 km/hr light rain condition (Fig. 6A). Steeper troughs with lower magnitude suggest that droplets were moving across the laser point quickly, evident in the 100 km/hr condition where droplets had higher kinetic energy. On the other hand, wider troughs seen in the 50 km/hr condition demonstrated the opposite for which droplets had higher adhesion at the contact interface with the cover surface.

Ultra-low distance (zero's) recorded may be contributed by a shorter time for the signal to return; in this case, it is hypothesized that a droplet was detected, and the droplet had a larger diameter such that all the signal was backscattered. Optical events such as reflection and refraction may have happened along the laser's path, the non-zero but lower than reference distances were consequences of two possible scenarios. First reason is due to detection of in-mid-air droplets. Another reason may be attributed to partial penetration of laser beam through a smaller droplet, and the cone-shaped beam with 2^{o} FOV detected a second object, such that a distance between the first and second detected objects was recorded.

Relative area under the curve of error count and error intensity was calculated for equally weighted increments, and the results for all investigated conditions are reported in Figure 7. The area determines the overall signal degradation of LiDAR. The bars represent the study group of perceived rain intensity. The LiDAR performance degraded when exposed to more raindrops. The arrows represent the study group of driving speed. Improvement was observed when driving faster, it was consistent for all three different perceived intensities. This was likely due to the narrow FOV of a single-point LiDAR, since a faster moving droplet would have a lower impact on signal accuracy.

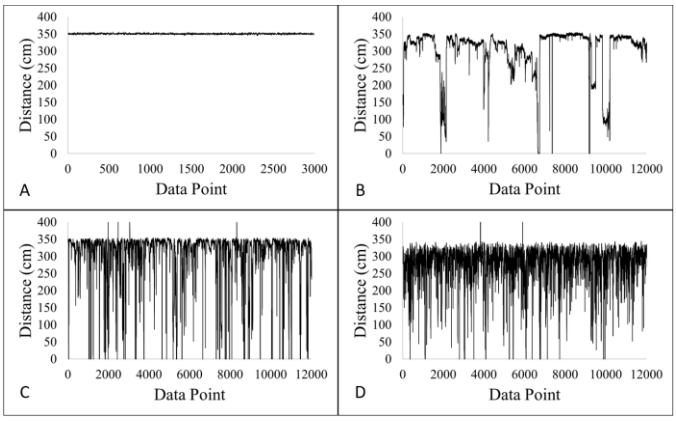

Figure 6. LiDAR distance measurements for (a) control, (b) 50 km/hr light rain, (c) 75 km/hr moderate rain, and (d) 100 km/hr heavy rain.

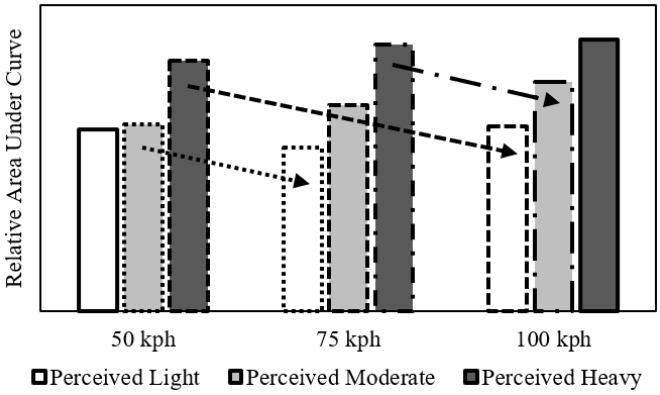

Figure 7. Relative area under the error frequency and intensity curve.

V. CONCLUSIONS

Realistic driving-in-rain conditions were simulated in a model wind tunnel. Two groups of conditions were studied – {1} driving at the same speed but experiencing different perceived rain intensities, and {2} driving at different speeds but experiencing the same perceived rain intensities. The effects of rain intensity and driving speed on signals of a generic automotive external camera and a single-point LiDAR were investigated and quantified via image processing and statistical analysis. The following conclusions were made:

- The camera performance degraded in terms of focus quality in both groups of conditions when rain intensity and driving speed increased.
- The LiDAR performance degraded with inaccurate ranging in group {1} conditions but showed opposite trend in group {2} conditions.

This paper serves as a baseline understanding for sensor behaviors when driving-in-rain, one of the most hazardous weather conditions, with several proposed methods to quantitatively analyze the effects of raindrops on sensor performances. The data analysis in this paper applies to the presented setup; whereas different setups may result in different conclusions. It is recommended to perform lab testing on signal strength to further understand other parameters such as droplet size and droplet shape. These studies can be used for future designs of soiling mitigation and signal enhancement strategies.

ACKNOWLEDGMENT

We acknowledge the support of the Natural Sciences and Engineering Research Council of Canada (NSERC).

REFERENCES

[1] P. Chazette, J. Totems, L. Hespel, J. Bailly, Principle and Physics of the LiDAR Measurement. N. Baghdadi, M. Zribi (Eds), Optical Remote Sensing of Land Surfaces. iSTE Press and Elsevier, 2016

[2] US Department of Transportation, "How do weather events impact roads?," [online] https://ops.fhwa.dot.gov/weather/q1_roadimpact.htm

[3] J. Qi, New Physics. Salt Lake City, UT: American Academic Press, 2018

[4] W. Y. Pao, M. Agelin-Chaab, "Fundamental and parametric considerations for numerical rain simulation in a wind tunnel", Progress in Canadian Mech. Eng., vol. 4, June 2021

[5] Bocci, F., "Whether or not to run in the rain", European Journal of Physics, vol. 33, no. 5, pp. 1321-1332, 2012

[6] M. Roser and A. Geiger, "Video-based raindrop detection for improved image registration," IEEE 12th Int. Conf. on Computer Vision Workshops, 2009, pp. 570-577

[7] M. Roser, J. Kurz, A. Geiger, "Realistic modeling of water droplets for monocular adherent raindrop recognition using Bézier curves," 2010 Asian Conference on Computer Vision (ACCV), pp. 235-244, November 2010

[8] H. Porav, T. Bruls, P. Newman, "I Can See Clearly Now: Image Restoration via De-Raining," 2019 Int.Conf. on Robotics and Automation (ICRA), pp. 7087-7093, 2019

[9] W. Y. Pao, L. Li, M. Agelin-Chaab, "A Soiling Mitigation Method to Enhance the Performance of ADAS in Precipitation", SAE technical paper, in press

[10] S. J. Yang, M. Berndl, D. M. Ando, M. Barch, A. Narayanaswamy, E. Christiansen, et al., "Assessing Microscope Image Focus Quality with Deep Learning," BMC Bioinformatics, vol. 19, no. 77, 2018

[11] M. Subbarao and J. K. Tyan, "Selecting the optimal focus measure for autofocusing and depth-from-focus," IEEE Transactions on Pattern Analysis and Machine Intelligence, vol. 20, issue 8, 1998

[12] H. Guan, N. Niinami, T. Liu, "Real-time object tracking for moving target auto-focus in digital camera," Real-Time Image and Video Processing 2015, vol. 9400, February 2015

[13] C. Goodin, D. Carruth, M. Doude, C. Hudson, "Predicting the influence of rain on LiDAR in ADAS," Electronics, vol. 8, no. 89, 2019

[14] A. Filgueira, H. Gonzalez-Jorge, S. Laguela, L. Diaz-Vilarino, P. Arias, "Quantifying the influence of rain in LiDAR performance," Measurement, vol. 95, pp. 143-148, 2017

[15] T. Fersch, A. Buhmann, A. Koelpin, R. Weigel, "The influence of rain on small aperture LiDAR sensors," 2016 German Microwave Conf. (GEMIC), pp.84-87, March 2016

[16] P. A. Lewandowsk, W. E. Eichinger, A. Kruger, W. F. Krajewski, "Lidar-based estimation of small-scale rainfall: empirical evidence," J. Atmospheric and Oceanic Technology, vol. 26, pp. 656-664, 2009

[17] C. Zhang, M. H. Ang Jr, D. Rus, "Robust LIDAR localization for autonomous driving in rain," 2018 IEEE/RSJ Int. Conf. on Intelligent Robots and Systems (IROS), Madrid, Spain: October 2018

[18] Thies Clima, Laser Precipitation Monitor, 5.4110.xx.x00, V2.5x STD, Instruction for use. Adolf Thies GmbH & Co. KG, Germany

[19] Fiji [online] https://imagej.net/software/fiji/